Environmental Toxicology and Pharmacology 94 (2022) 103903

Contents lists available at ScienceDirect

Environmental Toxicology and Pharmacology

journal homepage: www.elsevier.com/locate/etap

Evidences of the radiofrequency exposure on the antioxidant status, potentially contributing to the inflammatory response and demyelination in rat brain

Anjali Sharma [a,*,1], Sadhana Shrivastava [b], Asha Singh [b], Shamli S. Gupte [b], Arti Rathour [b], Mohd Salim Reshi [c], Sangeeta Shukla [b]

[a] Weill Cornell Medicine Helen & Robert Appel Alzheimer's Disease Research Institute, Feil Family Brain and Mind Research Institute, 413 E. 69th St., New York, NY 10021, USA
[b] UNESCO-Trace Element and Satellite Centre, School of Studies in Zoology, Jiwaji University, Gwalior, Madhya Pradesh 474011, India
[c] Toxicology and Pharmacology Lab, Department of Zoology, School of Biosciences and Biotechnology, Baba Gulam Shah University, Rajouri 185234, India

ARTICLE INFO

Edited by Dr. Malcolm D. Tingle

Keywords:
Inflammation
Electromagnetic radiations
Myelination
Brain
Oxidative stress

ABSTRACT

Present study exhibited the oxidative potential of microwave radiation (MWR) leading to the neurodegeneration in rats. *Wistar* rats were exposed at 2100 MHz frequency for 4 h/day, 5 days/week/3 months. Animals were exposed at an estimated specific absorption rate (0.453 W/kg) and power density (8.237 μW/m^2). After exposure irradiated group was compared with control group. Results indicated that microwave exposure significantly increased the levels of serological triglycerides and cholesterol. Oxidative stress is observed through alteration of glutathione homeostasis followed by activated inflammatory response further confirmed by pro and anti-inflammatory cytokines in the exposed group. Histopathological assessments and electron microscopic observation confirmed a significant change in the myelination pattern and cellular organelles in the brain of exposed animals. Taking everything into account it can be concluded that chronic exposure of 2100-MHz frequency caused oxidative stress, which leads to neural damage and demyelination and may affect neural communication.

1. Introduction

Radiation of all forms constitutes one of the environmental determinants of health and non-ionizing weak electromagnetic radiation is on of that. Electromagnetic field (EMF) is the combination of an electric and magnetic field and its natural sources play an important role in the functional activities of organisms (Juutilainen, 2003). Everyone is exposed to a complex mix of weak electric and magnetic fields, including sources such as mobile phones, telecommunications, and broadcasting installations. Telecommunications technology is expanding daily with 4G and upcoming 5G technologies. Globally, it is estimated that there are over 5.2 billion users of mobile phones, and this number will keep on growing (GSMA, 2020). Microwave radiation (MWR) exposure to humans has increased as a result of widespread usage of mobile phones. Microwave exposure leads to a potential DNA damage in brain and declines the cognitive function in rats (Deshmukh et al., 2016). Salford and the group also confirmed the brain damage, their study confirmed that mobile phone electromagnetic fields exposure causes neural damage in cortex, hippocampus and basal ganglia (Salford et al., 2003).

Pareja-Peña et al. (2020) found scientific evidence that reinforce causal association between electromagnetic field and brain tumor induction.

MWR excessively induces reactive oxygen species (ROS) (Oktem et al., 2005). ROS is linked to a variety of cellular pathologies, including inflammation, proliferation, and apoptosis (Yuan et al., 2016). Reactive oxygen species are the harmful reactive molecules (free radicals) generated by oxygen reduction (D'Autréaux and Toledano, 2007). The brain is a potential target of oxidative damage with its abundant fatty acids, high energy demand, and low antioxidant potential (Lakroun et al., 2015). Oxidative stress has been proven to promote cellular damage in neurological disorders (Fernandez-Fernandez et al., 2018). Reduced glutathione (GSH) is a major endogenous antioxidant that protects the organism against oxidative stress. Low GSH level can alleviate oxidative brain damage, thus plays an important role in the onset

* Corresponding author.
E-mail addresses: anjali.13809@gmail.com, anjali.noida11@gmail.com (A. Sharma).
[1] ORCID_ 0000-0003-4646-2668.

https://doi.org/10.1016/j.etap.2022.103903
Received 6 February 2022; Received in revised form 30 May 2022; Accepted 7 June 2022
Available online 11 June 2022
1382-6689/© 2022 Elsevier B.V. All rights reserved.

and progression of neuropsychiatric, neurodegenerative diseases and may be used as a biomarker for diagnosis. Oxidative stress leads to secrete various inflammatory cytokines that are responsible for glia cell activation as well as initiation and progression of neural damage (Spooren et al., 2011). Inflammatory cytokines and oxidative stress collectively involved in neuronal loss and finally cause cognitive deficits. On the other hand, it has been suggested that microwaves from the mobile phone, modify electrophysiological activity in the human brain and alter neurotransmission (Haghani et al., 2013). It is growing preclinical and clinical evidence that inflammatory cytokines play a central role in introduction of pathogenic neuroinflammation in Alzheimer's disease (Freeman and Ting, 2016).

Myelination is essential for fast signal propagation; proper myelination of axon is needed for rapid coordination of the brain, limbs, and sensory input. The myelin provides electrical insulation to the nerve fibers and is essential for the survival of neurons (Bhatheja and Field, 2006). Several neurological diseases are also associated with it, such as multiple sclerosis and chronic inflammatory demyelinating polyneuropathy that creates several motor and sensory disturbances (Wingerchuk et al., 2001). Since myelin greatly assists axonal integrity (Redmayne and Johansson, 2014), demyelination leads to alter nerve conduction by modifying the action potential and axonal loss (Griffiths et al., 1998). In our earlier study, it has been postulated that mobile phone radiation causes memory impairment, anxiety (Sharma et al., 2019), and all these symptoms are associated with demyelination (Redmayne and Johansson, 2014). Therefore, there is a possibility of electromagnetic field induces damage to the myelin sheath. Thus, the present study is designed to facilitate the information on the possible influence of EMR induced neurotoxicity, underlying the role of oxidative stress markers, which may be interconnected to antioxidant mechanisms, immune response, and myelination status.

2. Material and methods

2.1. Chemicals

The chemicals were analytical grade and purchased from Sigma Aldrich Company (USA) and E Merck (Germany). The other reagents used in the study were obtained from Ranbaxy and Rankem, Erba Pvt. Ltd. (India). Immunological estimations ELISA kits were procured from RayBio (USA).

2.2. Animals' maintenance

Seven weeks old Male *Wistar* rats, approximately 120 ± 10 g of body weight, were taken for the study. Animals were procured from the All-India Institute of Medical Sciences, New Delhi. All the animals were acclimatized to laboratory conditions for a minimum of 10 days before the experiments. Rats were housed under standard conditions (12-h light/dark cycle, 25 ± 2 °C temperature, and 60–70 % relative humidity) and kept in cages that have sterile bedding of paddy husk. Standard food pellets and clean drinking water were provided ad libitum. The experimental protocols were carried out according to the approved animal ethical guidelines set by the Institutional Animal Ethics Committee Jiwaji University (1854/GO/Re/S/16/CPCSEA/IAEC/JU/24).

2.3. Animal exposure

Animals were exposed to an experimental microwave exposure setup as described in our previous study (Sharma et al., 2019). The microwave exposure setup was designed for freely moving rats, possible to radiate homogeneously in the surrounding. The electromagnetic radiations were produced by rectangular microstrip patch antennas operated at 2100 MHz frequency band. The exposure setup is composed of two antennas (Transmitting and receiving antenna), a signal generator (ROHDE & SCHWARZ) and a spectrum analyzer (ROHDE & SCHWARZ FS315, 9 kHz to 3 GHz) designed at Madhav Institute of technology and Sciences, Gwalior, India. Animals were exposed to perforated polycarbonate cages (height–16, length–40, and width–24 cm), and placed in the exposure set up as described in our previous study (Sharma et al., 2020). Dosimetry characteristic of the radio-frequency antenna was expressed as power density and specific absorption rate (SAR). The value of specific absorption rate (SAR) was calculated from the electric field and tissue density (Panagopoulos et al., 2013), where the electric field was 17.660 V/m. The calculated SAR value of 2100 MHz is 0.453 W/kg with a maximum power level output of 2 W/kg and power density of 8.237 $\mu W/m^2$. Animals were exposed for 4 h a day, continually for five days in a week till three months.

Total 2 set of experiments were performed one is for histopathological and other is for biochemical analysis. Each set containing 20 animals so total 40 animals were used for both sets. Each experiment is divided into two groups (10 animals in each group). Group Ist (n = 10) served as a control group (sham-exposed) and group IInd (n = 10) was exposed to MWR.

Animals were exposed to MWR (4 h of exposure/day, 5 days in a week) constantly for 90 days at 2100 MHz frequency at the defined SAR and power density. Control group animals (sham-exposed) were kept in a similar condition without radiofrequency exposure.

2.4. Blood biochemistry

At the end of exposure tenure, rats were sacrificed, and the blood and tissue samples were collected. Serum was isolated from the blood samples by centrifugation at 2000 rpm for 15 min and was collected into vials to determine the levels of serum markers. The levels of TG, Cholesterol in the serum were determined by standard procedures used in clinical biochemistry laboratories based on manual biochemical kits following the manufacturer's directions (E-Merck Limited, India) using an auto-analyzer (Micro Lab 200, Merck, Germany).

2.5. Inflammatory assessments

The estimation of inflammation status was done through assessment of pro and anti-inflammatory markers such as interleukin-6 (IL-6, Lot# 0826160724), interleukin-10: (IL-10, Lot# 0812160704), and tumor necrosis factor-α (TNF-α, Lot# 0812160709) in the serum sample of the exposed animals. The estimation was based on the quantitative sandwich catalyst immunoassay through the standard procedure of Rat ELISA Kit, RayBio.

2.6. Indices of oxidative stress

The brain tissues were dissected out, rinsed in a cold 0.9 % sodium chloride solution, placed in pre-chilled homogenization buffers for further procedure. The oxidative status of the control and the exposed group was checked through various biochemical parameters in the brain tissue of the animals-

2.6.1. Reduced glutathione (GSH) and oxidized glutathione (GSSG) (Hissin and Hilf, 1976)

250 mg of tissue were homogenized in 3.75 ml phosphate EDTA buffer (0.1 M Sodium Phosphate Buffer containing 5.0 Mm EDTA, pH 8.0) and 1.0 ml of 25 % of HPO_3 which were used as protein precipitant. GSH or GSSG was assayed in supernatant obtained after centrifugation at 10,000 *g* for 30 min. 0.5 ml of supernatant was taken and 4.5 ml of phosphate EDTA buffer (pH 8.0) was added for estimation of GSH. The final reaction mixture contained 0.1 ml tissue supernatant, 1.8 ml PO_4 EDTA buffer and 10 μl of O-phthalaldehyd. Fluorescence was determined after 15 min of incubation (room temperature) at 412 nm with activation at 350 nm.

For the estimation of GSSG 0.5 ml of supernatant was taken and added to 0.2 ml of N-ethyl amide (NEM, 0.04 M) and incubated at room

temperature for 30 min to interact with GSH present in the tissue. To this mixture 4.3 ml of 0.1 N NaOH was added out of that 0.1 ml of aliquot was taken and used for GSSG assay in the manner identical to GSH except 0.1 N NaOH was employed as diluents in place of phosphate EDTA buffer. Both GSH and GSSG standard curve were prepared in a similar manner using concentration range 20–100 μg. The unit of measurement was expressed as GSH, GSSG μg/g tissue[1].

2.6.2. GSH cycle enzymes

Glutathione reductase (GR) was estimated by measuring the conversion rate of NADPH to NADP. 10 % homogenate was prepared in 1.15 % KCl and centrifuged for 10 min at 10,000 rpm.

2.6.2.1. Glutathione reductase (Tayarani et al., 1989). Previously prepared supernatant was taken for the test. The reaction mixture consists of 0.7 ml phosphate buffer, 0.1 ml homogenous and 0.1 ml oxidized glutathione. Then it was incubated at room temperature for 10 min. NADPH (0.1 ml) was introduced to initiate the reaction. Absorbance change/ min recorded at λ 340 nm for 5 min. Specific activity was expressed in the term of μ mol NADPH oxidized/min/mg protein taken as the extinction coefficient of NADPH as 6300 m^{-1} cm^{-1}.

2.6.2.2. Glutathione peroxidase (Paglia and Valentine, 1967). A mixture was produced by adding 0.05 ml homogenate with a reaction mixture contained 0.05 ml sodium azide, 0.3 ml sodium phosphate buffer, 0.01 ml NADPH, 0.1 ml reduced glutathione, and 0.05 ml glutathione reductase further incubated for 10 min at room temperature. Reaction was initiated after adding 0.05 ml H_2O_2 and change in optical density/minute was documented for 5 min at λ 340 nm. μmol NADPH oxidized/min/mg protein was expressed as a specific activity of NADPH as 6300/m/cm.

2.6.2.3. Glutathione-S-transferase (Habig et al., 1974). Reaction mixture is made up with 0.5 ml phosphate buffer and 50 μl of CDNB. 50 μl homogenate was added to the reaction mixture and then incubated at room temperature for 10 min, then 25 μl of GSH was added to start the reaction and change in the optical density per minute was documented for 5 min at λ 340 nm.

2.6.2.4. Glucose-6-phosphate dehydrogenase (Askar et al., 1996). The reaction mixture containing 0.1 ml $MgCl_2$, 0.1 ml glucose-6-phosphate, 1.5 ml tris HCl buffer, 1.0 ml distilled water and 0.1 ml diluted sample and then incubated for 10 min at room temperature. 0.2 ml $NADP^+$ was added to initiate the reaction of the mixture and change in absorbance/minutes was recorded for 5 min continuously at λ 340 nm. Specific activity was expressed in term of μ mol NADPH formed min^{-1}/mg^{-1} protein by the motor extinction coefficient of NADPH as 6300 m^{-1} cm^{-1}.

2.6.2.5. Adenosine triphosphatase (Seth and Tangri, 1966). Adenosine triphosphatase (ATPase) was determined by the addition of 0.05 ml homogenate, 0.2 ml of tris buffer, 0.2 ml of 0.1 M ATP and 1.55 ml of distilled water. This mixture was then incubated at 37 °C for 15 min. The reaction was stopped by adding 1 ml of 10 % TCA which was further centrifuged at 2000 rpm to collect the supernatant. 2 ml of supernatant was mixed with 6.6 ml distilled water and 1 ml of ammonium molybdate to initiate final reaction through 0.4 ml ANSA. Change in the absorbance was recorded at λ 620 nm in the unit mg pi/100 g/min.

2.6.2.6. δ-aminolevulinic acid synthase (Maines, 1980). This method was employed to calculate the brain δ-aminolevulinic acid synthase (ALAS). Brain homogenate (0.3 ml) was made in 0.05 M Tris chloride buffer, with pH 7.4 and then added to 1.7 ml of reaction cocktail. Tubes were incubated for 60 min with temperature 37 °C. The reaction was put at halt by adding 1 ml of 10 % TCA. The samples were then centrifuged at 3000 rpm for 15 min to collect the supernatant. Further 0.5 ml of supernatant was taken and mixed with 0.2 ml of acetylacetone and then kept in boiling water bath for 5 min. Lastly Ehrlich's reagent (0.5 g dimethylaminobenzaldehyde in 12.5 ml acetic acid + 6 ml of perchloric acid + 2.5 % 1 ml $HgCl_2$) was proportionately added and absorbance was reported and calculated at 555 nm.

2.6.2.7. δ aminolevulinic acid dehydratase (Berlin and Schaller, 1974). Berlin and Schaller (1974) method are applied to evaluate the functioning of blood δ aminolevulinic acid dehydratase (ALAD). The sample mixture contains 0.2 ml of heparinized blood and 1.3 ml of DH_2O and incubated for 10 min at 37 °C for complete hemolysis. 1 ml of standard aminolevulinic acid was supplemented to the tubes and further incubated for 60 min at 37 °C. The reaction was stopped with 1 ml of tri-chloro acetic acid (TCA) after 1 h. The samples were centrifuged again at 3000 rpm for 15 min to collect the supernatant and proportionate volume of Ehrlich's reagent was added to it. The absorbance was calculated at 555 nm after 5 min.

2.7. Histopathological observations

2.7.1. Light microscopic studies

A set of experiment was performed for histopathological observations. The transcardial perfusion procedure was performed with PBS (0.01 M; pH 7.4) to obtain the best possible preservation of the brain in a controlled and uniform fixation procedure using 4 % paraformaldehyde in 0.01 M PO^4 buffer (pH 7.4). After the sacrifice, the brain was isolated and different parts of the brain (Hippocampus, Cerebellum, Corpus Callosum & Striatum) were instantly dissected out into small pieces. Fixed tissues were processed for paraffin sectioning as per the previously described method (Kesari et al., 2011). Briefly, after fixation, tissues were carefully washed with water and dehydrated with a graded series of ethyl alcohol. Then, the tissues were cleared in toluene and infiltrated in paraplast (Sigma, m. p. 56–58 °C) for proper impregnation of wax. Tissue blocks were made in the paraffin and serial coronal sections of the hippocampus were cut at a thickness of the 10 μm using WESWOX-MT1090A microtome. Paraffin sections from both exposed and control groups were randomly selected, dehydrated, and stained with Luxol Fast Blue (0.1 g Luxol fast blue from Sigma Aldrich, USA in 100 ml of 90 % ethanol with 10 % Glacial acetic acid) and Cresyl Violet stain. The differentiation of the gray and white matter tissue was obtained with lithium carbonate (0.25 g in 250 ml of double-distilled water) followed by counterstaining with Cresyl Violet (Sigma Aldrich, USA C-1791). These sections were finally mounted in DPX (Clarke, 1984). Pathological modifications of the sections were investigated under the Leica DM LB microscope and the image acquisition was done with a Leica digital camera (DC) 500 attached to Qwin V_3 software.

2.7.2. Ultrastructure changes

In electron microscopic studies, section (1 mm^3) of neural tissues was immediately fixed in Karnovsky solution followed by phosphate buffer washing, after washing tissues were post-fixed with 1 % osmium tetroxide and again washed three times with phosphate buffer. Tissues were then dehydrated in the acetone series followed by toluene clearance (2 changes 30 min each). These tissues were further embedded into resin to form blocks and then these blocks were cut into ultrathin sections (~ 70 nm) with a model MT-X ultra-microtome (RMC, Tucson, AZ) and collected on copper grids. These sections were stained with uranyl acetate, lead citrate, and observed using 5022/22 Tecnai G2 20 S-Twin (Czech Republic) electron microscope with digital micrograph software (Hayat and Giaquinta, 1970).

2.8. Statistical analysis

Data were statistically expressed as mean ± S.E. (n = 10), the difference between, control and exposed groups were measured by the

Student's 't' test, at their respective P-values. Statistical analysis was performed using GraphPad InStat 3.10 software package.

3. Results

3.1. Blood and serum biochemical variables

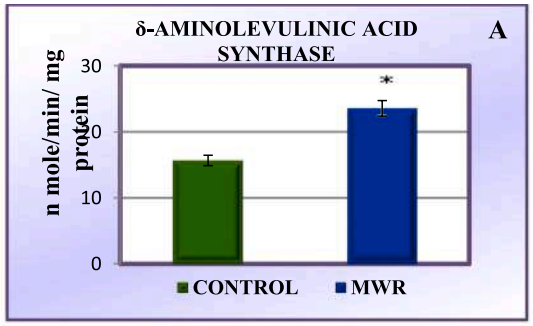
δ Aminolevulinic acid synthase (ALAS) is an enzyme that catalyzes the synthesis of δ-aminolevulinic acid (ALA) the first common precursor in heme synthesis. An increase in the ALAS production impaired heme synthesis. Long-term exposure showed a significant increase in the ALAS level ($P = 0.0003$) compared to the control group as depicted in Fig. 1**A**.

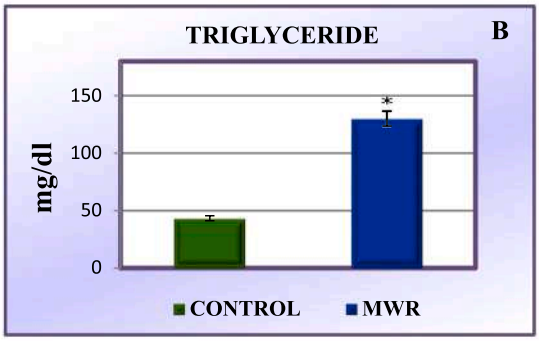
Triglycerides are necessary for certain cell functions; higher levels of triglycerides and cholesterol can cause serious health problems. Fig. 1**B–C** illustrated how microwave exposure alters the plasma lipid profile through serum triglycerides (Fig. 1**B)** and cholesterol **(**Fig. 1**C).** Potentially elevated cholesterol and triglycerides were seen in exposed group animals when compared with the control group ($P < 0.0001$). Fig. 2**A** depicts the blood ALAD activity. The inhibition of ALAD averts the conversion of ALA to porphobilinogen, which impaired heme synthesis. Long-term exposure showed a significant fall in the δ Aminolevulinic acid dehydratase (ALAD) level in the blood, which may decline the hemoglobin content in exposed animals. Fig. 2**B** presented the influence of microwave exposure on the activity of the adenosine triphosphatase (ATPase) enzyme. The result demonstrated significant depletion in the enzymatic activity of ATPase due to microwave exposure while the control group showed normal ATPase activity ($P < 0.0001$).

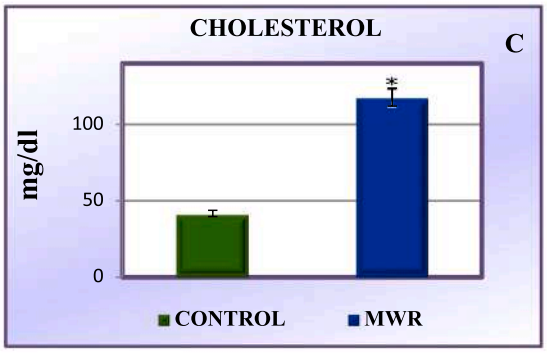
3.2. Oxidative stress and cellular antioxidant pool

3.2.1. Reduced glutathione and oxidized glutathione (GSH/GSSG)

Cellular oxidative stress is a measure of the reduced glutathione (GSH) to oxidized glutathione (GSSG) ratio in the cell. MWR exposed animals showed a 29 % decrease in the GSH content compared with the control group. Chronically exposed animals showed a significantly marked increase in the levels of GSSG and the increase observed was 59 % when compared with control **(**Table 1**).** A considerable change in the GSH/GSSG ratio was observed in the brain after MWR exposure (Table 1**).** The variance between both the groups was found to be significant when analyzed by the student's t-test ($P < 0.0001$).

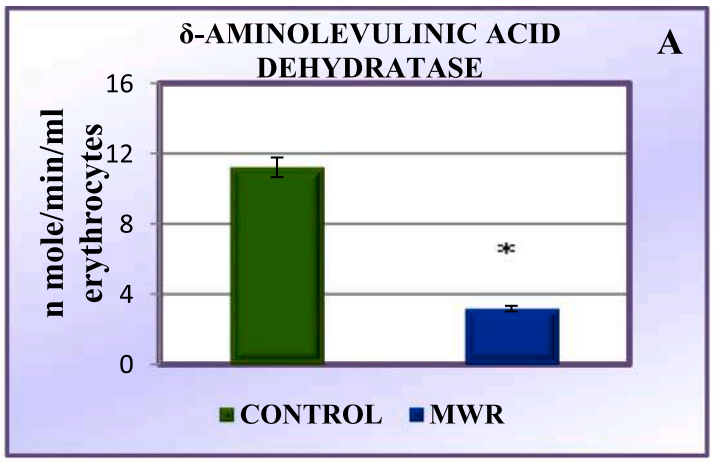


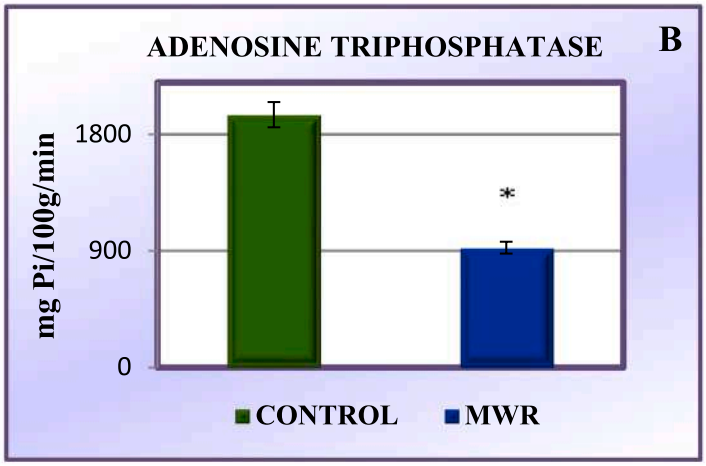




F value (at 5% level)	ALAD	TG	CHOL
	29.20@	28. 90@	51.11@

Fig. 1. Microwave association with transaminases and ALAS serum lipid profile. Data are mean ± S.E.; N = 10; * MWR vs Control at $P < 0.0001$. Abbreviations: ALAD = δ-aminolevulinic acid dehydratase; TG: Triglycerides CHOL: Cholesterol.





F value	ATPase	ALAD
(at 5% level)	44.61@	20.30@

Fig. 2. Effect of MWR on tissue biochemical parameters. Data are mean ± S.E.; N = 10; * MWR vs Control at P < 0.0001 (ATPase), P = 0.0003. (ALAS). Abbreviations: MWR = Microwave radiation; ATPase = Adenosine triphosphatase; ALAS = δ-aminolevulinic acid dehydratase.

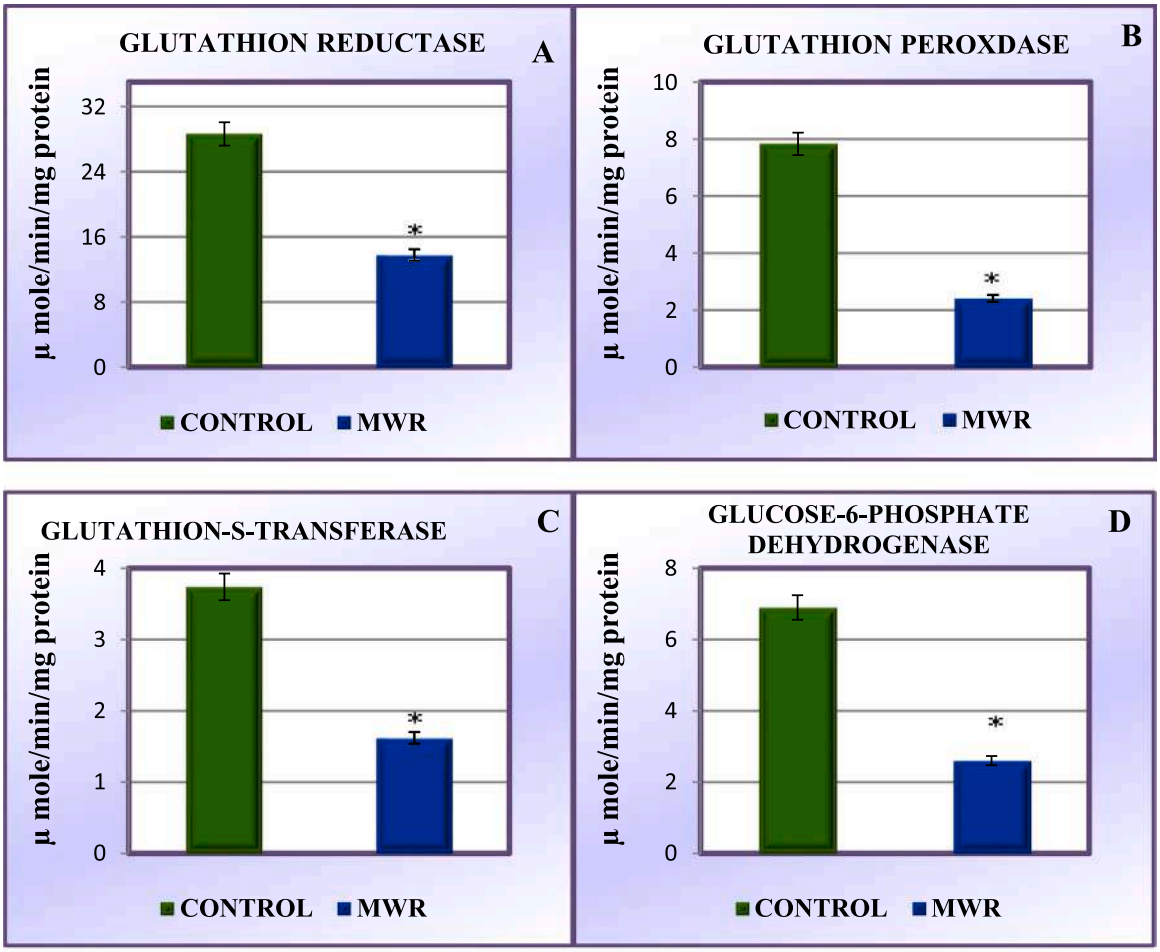
Table 1
Effect of microwave exposure on the level of GSH, GSSG, and GSH/GSSG ratio of the rat brain.

Parameters	Control	MWR exposed
GSH	***226.31*** ± 11.421	***161.38*** ± ***8.144**** ***(29 %)***
GSSG	***115.49*** ± 5.828	***282.17*** ± 14.240* ***(59 %)***
GSH/GSSG ratio	***1.96***	***0.571***
	GSH	**GSSG**
F value (at 5 % level)	***1.967***@	**5.969**@

GSH and GSSG levels are expressed as $\mu g/mg^{-1}$ tissue. Data are mean ± S.E.; N = 10; * MWR vs Control at P < 0.0001 (GSSG), P = 0.0009 (GSH).
Abbreviations: MWR = Microwave radiation; GSH = Reduced glutathione; GSSG = Oxidized glutathione.

3.3. Effect on the enzymes of GSH cycle

The glutathione redox cycle is a mechanism that maintains the GSH pool and scavenges lipid peroxides and hydrogen peroxide through reduced glutathione. Fig. 3 demonstrates the effect of MWR on GSH cycle enzymes. Glutathione reductase (GR) is used for the maintenance of normal GSH levels in the body concerned with the conversion of GSSG into GSH by affecting the fast reduction of oxidized glutathione to the reduced form. A significant inhibition in the activity of the GR enzyme is found after microwave exposure Fig. 3**A** (P < 0.0001). Glutathione peroxidase (GPx) removes hydrogen peroxides (H_2O_2) generated by superoxide dismutase in the cytosol and mitochondria of the cells. MWR exposure significantly inhibited the enzymatic activity of GPx in the brain (Fig. 3**B)** (P < 0.0001). Glutathione-S-transferase (GST) catalyzes the conjugation of GSH with toxic compounds, thus the couple of GSH with GST acts as a significant protection component of cellular defense against toxic electrophiles. Exposure of microwave frequency showed a prominent fall in GST activity of the exposed group concerning to their control values as depicted in Fig. 3**C.** The significance of the results was determined by the student t-test. Glucose-6-phosphate dehydrogenase (G6PDH) is responsible for the production of NADPH required in the regeneration of GSH. Fig. 3**D** clearly showed a significant (P < 0.0001) inhibition of G-6PDH activity after 90 days of exposure at 2100 MHz frequency, while the control group showed normal levels of G-6PDH (P < 0.0001).



F value	GR	GPx	GST	G6PDH
(at 5% level)	48.34[@]	10.52[@]	53.30[@]	70.26[@]

Fig. 3. MWR toxicity on glutathione homeostasis. Data are mean ± S.E.; N = 10; *MWR vs Control at P < 0.0001. Abbreviations: MWR = Microwave radiation; GR = Glutathione reductase; GPx = Glutathione peroxidase; GST = Glutathione-S-transferase; G6PDH = Glucose-6-phosphate dehydrogenase.

3.4. Inflammatory cytokines (IL-6, IL-10, and TNF-α)

Cytokines are small, non-structural proteins having a complex regulatory effect on inflammation and immunity. Secretion of pro and anti-inflammatory cytokines defines the inflammatory status of the body. Chronic MWR exposure significantly increased the level of pro-inflammatory cytokines such as IL-6 (Fig. 4**A**), TNF-α (Fig. 4**B**) in the blood while decreasing the level of anti-inflammatory cytokines such as IL-10 (Fig. 4**C**) (P < 0.0001).

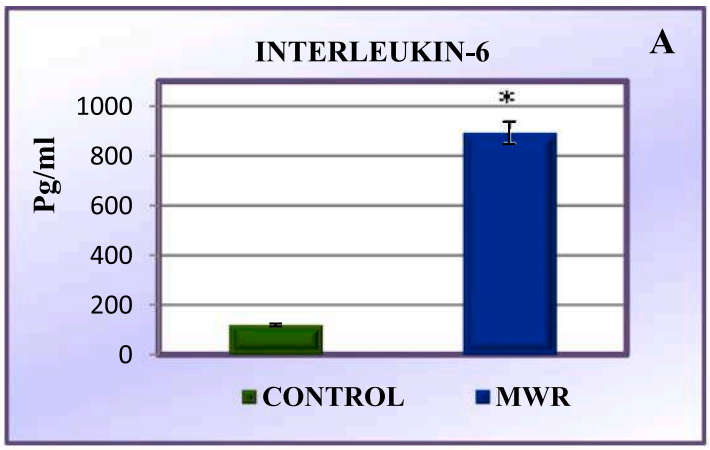
3.5. Histopathological observations

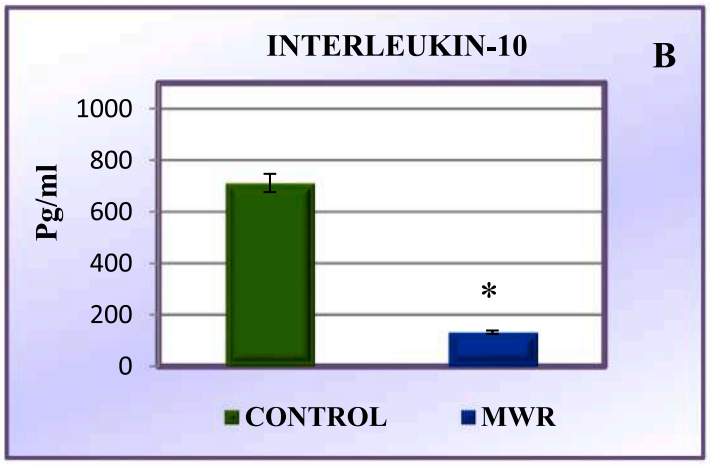
3.5.1. Light microscopy

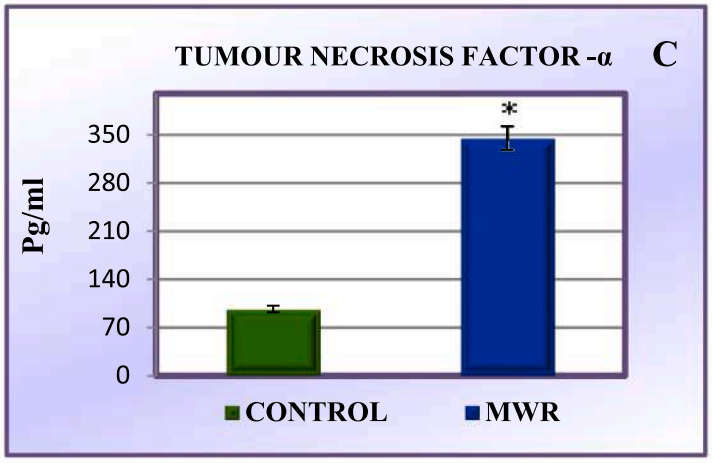
3.5.1.1. Hippocampus. The hippocampus area was assessed through cresyl violet (CV) stain. Microwave exposure shunts the normal features of the brain after 90 days of chronic exposure. Animals of the control group showed densely packed, large vesicular nuclei in the pyramidal neurons of cornu ammonis (CA) and dentate gyrus (DG) regions (Fig. 5**A**). Magnified images of the control group showed well-formed pyramidal neurons in CA1 (Fig. 5**B**), CA2 (Fig. 5**C**), CA3 (Fig. 5**D**), and DG (Fig. 5**E**) region of the hippocampus. An evident increase of degenerated cells was detected in the hippocampus of exposed animals as showed in Fig. 5**F**. Prominent darkly stained pyramidal cells with degenerated pyknotic nuclei were depicted in the CA1 (Fig. 5**G**), CA2 (Fig. 5**H**), CA3 (Fig. 5 **I**), and DG (Fig. 5**J**) regions due to MWR exposure.

3.5.1.2. Cerebellum. Cerebellum region was stained with luxol fast blue to observe molecular, Purkinje, and granular neuron layers as depicted in Fig. 6**A**. Control group animals showed well-formed Purkinje neuron with long dendrites processes (Fig. 6**B**). Animals exposed to microwave showed degenerated Purkinje cells having condensed nucleic material and short dendritic processes (Fig. 6**C**).

3.5.1.3. Corpus callosum and striatum. The forebrain comprised most of the white matter, including the fiber tracts of the cerebral cortex and corpus callosum. The corpus callosum is the largest white matter structure, which links two hemispheres and subcortical tracts of the limbic system. The effect of microwave exposure was studied by staining the white matter with luxol fast blue. The control rat's brain has typical histological characteristics, including a corpus callosum with well-formed myelination thickness. The striatum was found to have evenly distributed myelin intensity, followed by healthy neuron and neuroglia cells in the cauda putamen, corpus callosum, and thalamus regions







F value	Il-6	Il-10	TNf-α
(at 5% level)	54.40[@]	33.28[@]	12.83[@]

Fig. 4. Inflammatory response due to MWR exposure. Data are mean ± S.E.; N = 10; * MWR vs Control at P < 0.0001. Abbreviations: MWR = Microwave radiation.

(Fig. 7**A–C).**

Microwave exposure damaged the cytoarchitecture of the corpus callosum. Exposed animals showed mild staining of white matter; thus, it was evident that there was a consistent reduction in white matter density, with other deformities like depressed, fragmented thinner fibers with poor margins. Fig. 7**D** depicts reduced myelination thickness in the corpus callosum. A decrease in the myelin intensity and cellular debris was observed in the border zone of peri-infarct areas of the striatum **(**Fig. 7**F).** The appearance of neuroglial cells with pericellular halos and vacuolization was confirmed; however, cell density was also decreased in the cauda putamen, corpus callosum, and thalamus region **(**Fig. 7**D-F).**

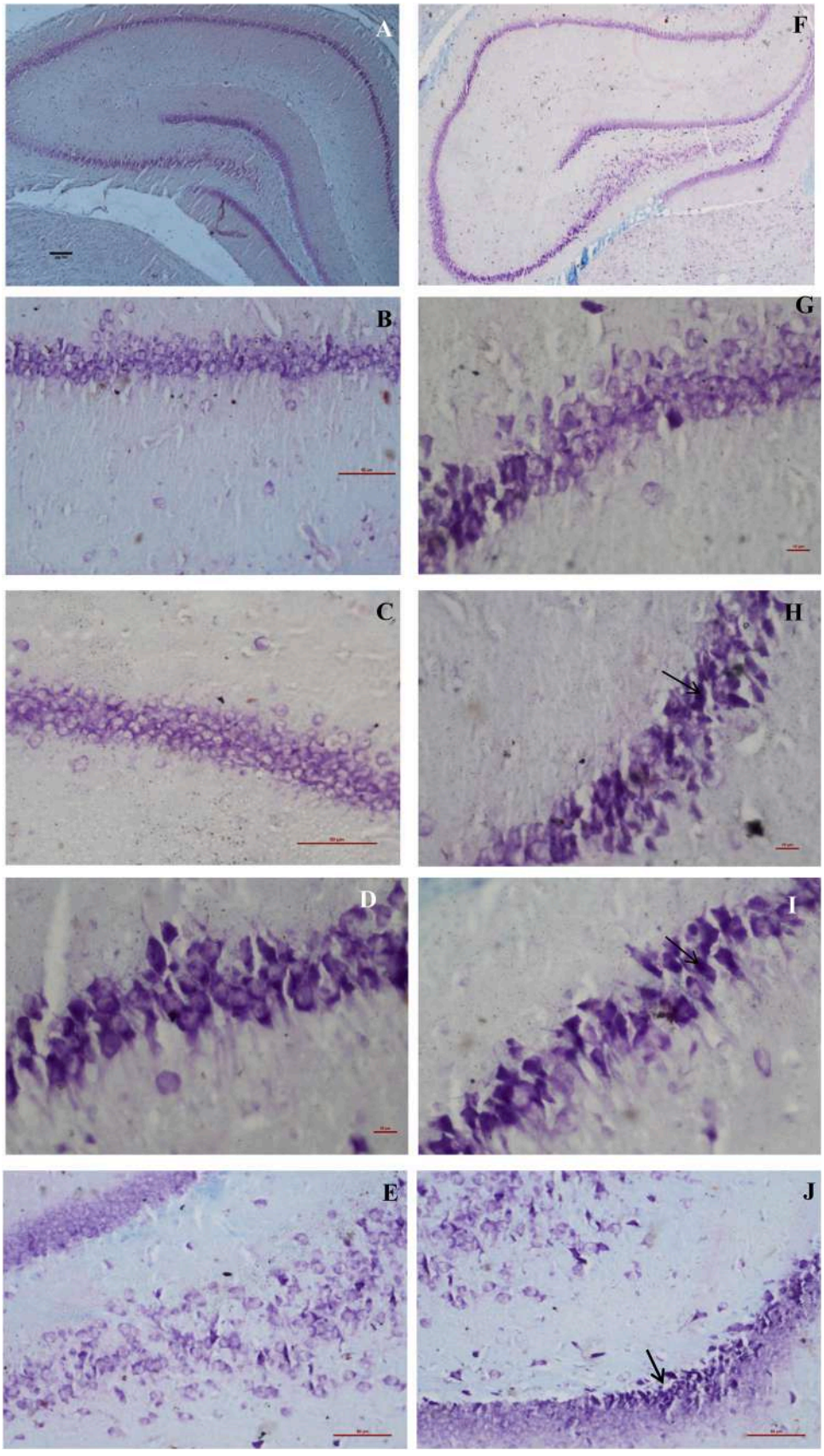


Fig. 5. Effect of MWR exposure on Hippocampus. A: Cresyl violet stains of control rat hippocampus. **B:** Hippocampus proper of Exposed group **(× 100). C–E:** Brain of control rat showing well-formed neurons, with healthy pyramidal neurons (Py) in CA1, CA2 and CA3 region. **G–I:** Exposure of MWR showed degenerated pyramidal cell neuron in the hippocampus region with significant pyknosis (PK) in pyramidal (Py) cell neuron of CA1, CA2 and CA3 regions. **F:** DG region of control group showing healthy granular neuron layer. **J:** Exposure of MWR caused darkly stained, shrunken, pyknotic neuron cells with dense, hyper chromatic nuclei **(× 400).**

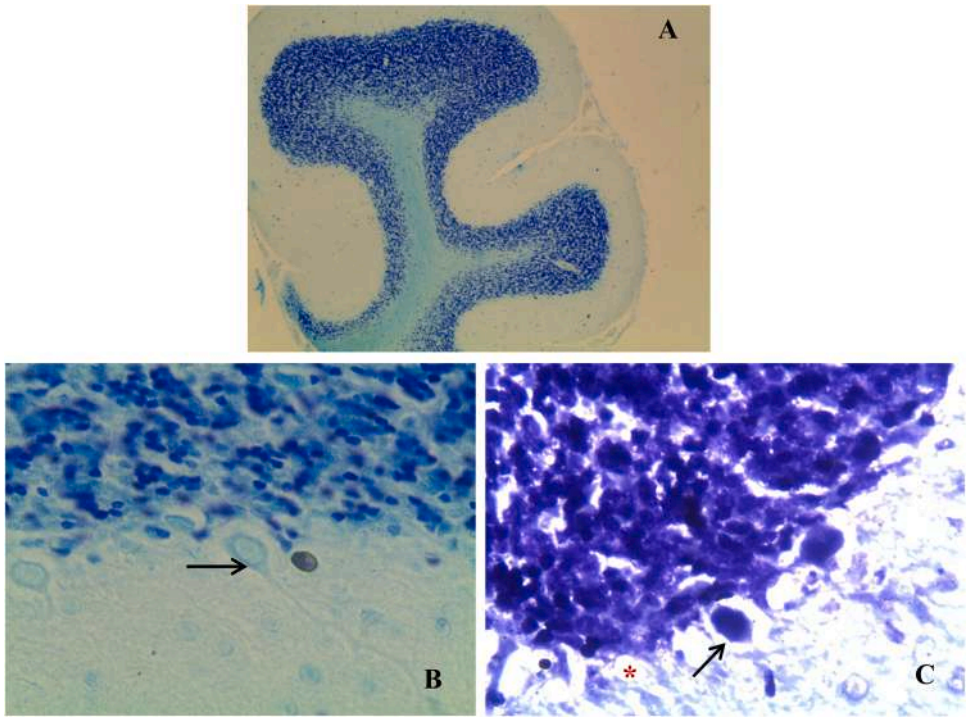


Fig. 6. Effect of MWR on cerebellum. A: Cerebellum region showed Purkinje (Pu) granular (G) and molecular (M) neuron layer **(× 100). B:** Control group showed healthy Purkinje cells with long dendritic processes, **C:** In case of microwave exposure degenerated dendritic processes with condensed nucleic material was observed **(× 1000).** Free spaces showed neural loss as depicted by (*).

3.5.2. Transmission Electron Microscopy

The ultrathin sections of brain were observed through electron microscope with digital micrograph software. The brain of the control rat illustrated; well-formed nucleus covered with an intact nuclear envelope. Nucleolus was densely stained by the presence of clear neurofilaments (euchromatin and heterochromatin) as depicted in Fig. 8**A.** Observations showed well-maintained endoplasmic reticulum (rER and sER) and mitochondria with prominent cristae. Axons of control animals have evenly distributed neurofilaments, profuse number of synaptic connections, and a large number of synaptic vesicles at both pre- and post-synapse axon terminals **(**Fig. 8**B–E).** The control group showed dense and properly stacked, darkly stained compact myelin fiber. For more clarity quantitative assessment of relative myelination in the axons was observed, at higher magnification (50,000 ×). The control group showed properly stacked compact and thick axonal myelination (111.67 ± 5.4 nm width in diameter) (Fig. 8**F**).

The brains of microwave exposed animals showed ultra-structural modifications. Cytoplasmic fragments and scattered nerve filaments were noticed with many inclusions (Fig. 9**A**). The nucleus was shrunken darkly stained, encircled by an unclear nuclear membrane. Highly electron-dense nucleoplasm was observed with irregularly dispersed chromatin material such as euchromatin (Eu) and heterochromatin (Hc) (Fig. 9**A–B**). Sections of the brain showed degenerated granular reticulum, Golgi bodies and the presence of autophagosomes. The perikaryal cytoplasm of these cells consisted of a relatively thin rim containing few organelles as compared to control animals. MWR exposure also resulted in mitochondrial swelling and disintegrated cristae. In the synaptic morphology, we have found loosely connected terminal synapses with less dense synaptic junctions and a lack of synaptic vesicles **(**Fig. 9**C).** MWR exposed animals showed the formation of inflammasome due to induction of the inflammatory process (Fig. 9**D–E).** Exposure also caused disorganized, deteriorated, and thinner myelin compaction (76.99 ± 6.66 nm) of axons with irregularly arranged wavy myelin sheath (50,000 ×) (Fig. 9**F**).

4. Discussion

Excessive usage of mobile phones has resulted in a significant increase in the prevalence of neurotoxicity (Bandara and Carpenter, 2020; Pareja-Peña et al., 2020). Previous literature suggests that chronic exposure to RF-EMR showed impact on amygdala cellular architecture, place preference and hyperactivity-like behavior in rats (Narayanan et al., 2018). Faridi and Khan (2013) confirmed the electron-microscopic morphological alterations in sector CA3 of hippocampus which may in long term, lead to both cognitive and behavioral changes.

Chauhan et al., 2017 also confirmed that exposure to microwave radiation (2.45 GHz) 2 h a day for 35 days can potentially cause histopathology and oxidative changes in *Wistar* rats. They observed histological changes in the brain, liver, testis, kidney and spleen after whole-body microwave exposure (Chauhan et al., 2017). RF-EMR exposure for 2 h/day for 30 days induces poor spatial memory performance and lead to morphological changes in the CA1 region of hippocampal such as degeneration of mitochondria and shorter postsynaptic densities in the rats (Li et al., 2012). In another study, it was found that, Mobile phone RF-EMR exposure for a month induced altered passive avoidance behavior and hippocampal morphology in rats (Narayanan et al., 2010). There are so many more studies in support of above studies, so the MWR and its biological effects have been a burning topic of discussion and research in recent years.

Mobile phone radiation even in the permissible range when used for longer duration causes significant genotoxicity (Banerjee et al., 2016). According to the studies, there is a dosimetric relationship between the mobile phone exposure and its consequences. Previous research has also confirmed that there is a substantial link between mobile phone use (for more than 10 years and more than 74 h of accumulated use) and the appearance of different malignancies (Pareja-Peña et al., 2022). Another study noted a positive correlation between the duration of semen samples placement in the vicinity of mobile phone electromagnetic radiation and the level of DNA fragmentation: the longer the exposure period, the

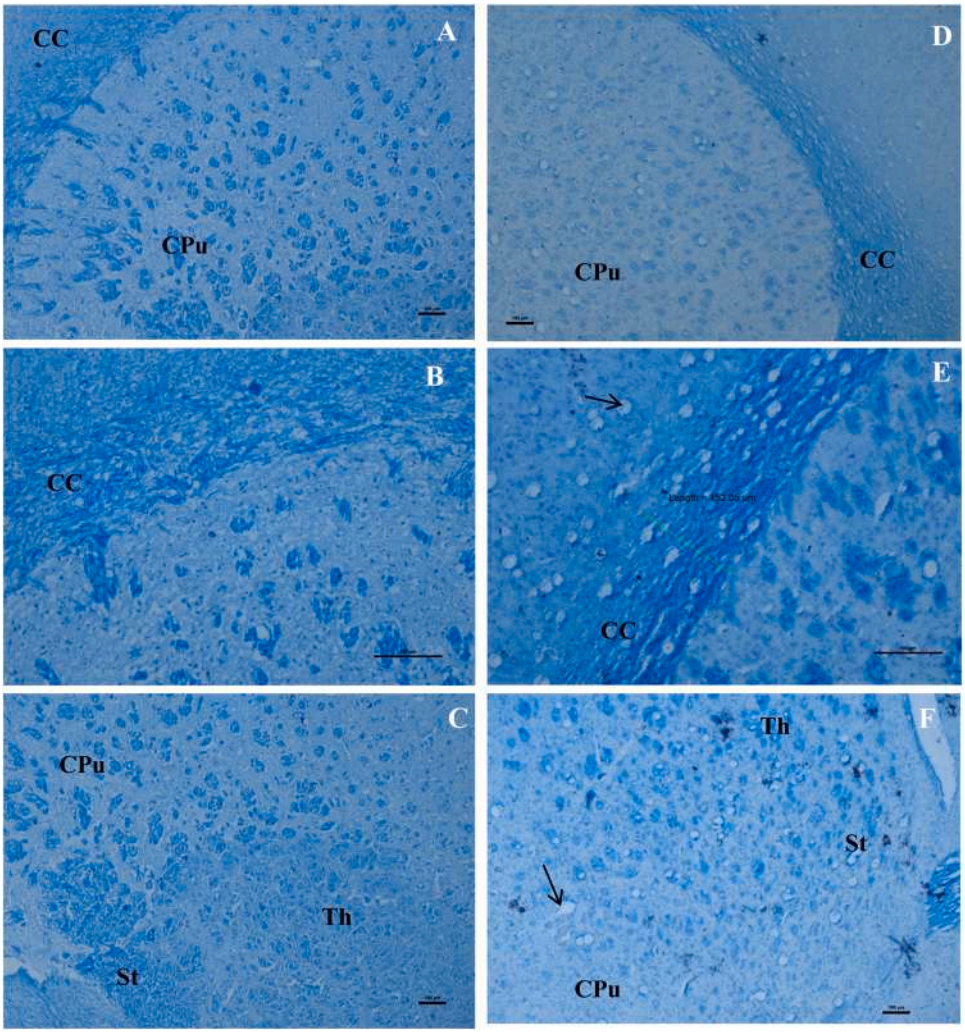


Fig. 7. Effect of MWR on corpus callosum and striatum region. A–C: Luxol fast blue stain of the control rat brain reveals normal histological features with well form myelination thickness in the corpus callosum (CC). Equally distributed myelin (My) intensity in the striatum region (St). Healthy neuron and neuroglia cells observed in the cauda putamen (CPu), CC, thalamus (Th) region of the brain of control animals **(× 100, 400). D–F:** Microwave exposure at 2100 MHz showed reduced myelin thickness in the corpus callosum (CC) and striatum region (St). Neural damage and cellular debris were observed in the border zone of peri-infarct areas of striatum. Appearance of neuroglia cells with pericellular halos and vacuolization were found however, cell density was also decreased in cauda putamen (CPu), corpus callosum (CC) and thalamus region (Th) **(× 100, 400).**

more frequent DNA damage occur (Gorpinchenko et al., 2014). Thus Keeping in mind that mobile phone exposure has a dosimetric effect, we chose a longer exposure hour (4 h/day) for a chronic duration to check its maximum potential consequences. We have selected the frequency (2100 MHz) according to our previous research we have checked different frequencies and found that 2100 MHz frequency is causing more harmful effect as compare to the lower frequencies (Sharma et al., 2021).

Results of the present study demonstrated that MWR mediated oxidative stress in rats was associated with metabolic and morphological aberrations in the brain. The results were in support of the previously done in vivo studies (Volkow et al., 2011; Zymantiene et al., 2020) suggested that the chronic exposure of MWR exerts neuronal damage. Lipid imbalances in the central nervous system may cause functional changes, which can lead to disorders like Alzheimer's, Huntington's, and Parkinson's (Adibhatla and J.F.H., 2007). Impairment in the crucial cellular process might exist due to an increased level of TBARS, an indicator of lipid peroxidation (Sharma et al., 2017). This fact was also well supported by our previous study, which showed changed brain lipid metabolism as a result of MWR exposure (Sharma et al., 2019; Martínez-Sámano et al., 2018). ATPase is a mitochondrial lipid-dependent membrane-bound enzyme. Any alteration in membrane lipid leads to a change in membrane fluidity, which in turn alters the ATPase activity and cellular function. The main function of this enzyme is to maintain the balance in the plasma membrane through an active transport system. Microwave exposure caused a significant decrease in ATPase activity (Brown and Chattopadhyay, 1991). Loss of ATPase might hamper the energy conservation, active transport and pH homeostasis so that neural cells could not function properly (Ravikumar Kurup and Parameswara Achutha, 2012).

Serum cholesterol and triglyceride have also been assessed in the MWR exposed animals. Our finding supports the previous studies that chronic exposure increased the level of serological TG and cholesterol (Israel et al., 2007). Elevation in cholesterol level may be due to increased liver fatty acid synthesis. The elevated levels of total cholesterol and triglycerides in the blood plasma are most likely caused by the higher levels of VLDL-c, which may be linked to cardiovascular problems due to RF-EMR (Ismaiil et al., 2019).

Microwave exposure significantly alters the key enzymes such as ALAD, ALAS involved in heme synthesis and ultimately alters the heme synthesis pathway. ALAS is a mitochondrial enzyme; it catalyzes the condensation of glycine and succinyl CoA to form ALA. Chronic MWR exposure inhibits this rate-controlling step that is a highly regulated reaction in heme biosynthesis. MWR induces the inhibition in ALAD, resulting in the accumulation of δ- aminolevulinic acid (ALA). Due to this ALA is not able to convert into porphobilinogen which inhibits the incorporation of iron into the protoporphyrin ring and ultimately impaired the pathway for heme synthesis (Jangid et al., 2012). Accumulation of ALA is a potential source of reactive oxygen species (Kumar et al., 2012). This accumulated δ-ALA by the process of enolization and auto-oxidation enhanced reactive oxygen species, which might a possible cause of MWR induced neurological disturbances (Gurer-orhan

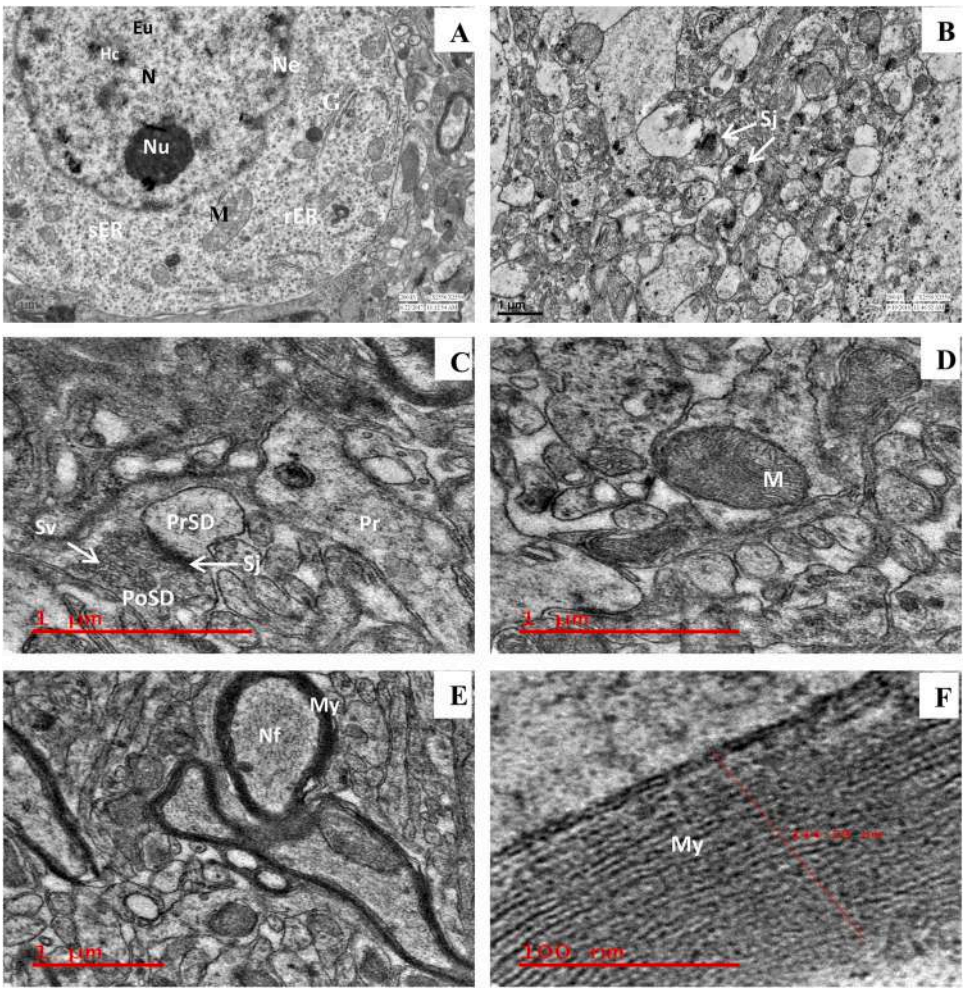


Fig. 8. Electron micrographs of control group animals. A–F: Electron micrographs of control brain showed well-formed nucleus (N) with dense nucleolus (Nu), presence of clear neurofilaments (Nf), intact nuclear envelope (Ne), rough endoplasmic reticulum (rER), smooth endoplasmic reticulum (sER), Golgi bodies (G) and healthy mitochondria (M). Myelinated (My) axons, an abundant number of synaptic junctions (Sj) and neural processes (Pr) were appeared. Rich numbers of synaptic vesicles (Sv) at axon terminals were observed in the pre (PrSD) and post synaptic density (PoSD) of the axon synapses. Protein rich, equally distributed dense neurofilaments (Nf), properly stacked myelin sheath (Ms) of myelinated axon was also observed.

et al., 2004).

Glutathione metabolism is one of the most essential processes of antioxidative defense mechanisms which scavenge lipid peroxides and H_2O_2. The continuous reduction of GSSG by NADPH and GR keeps cellular GSH levels in check. The GSH/GSSG ratio is very important for maintaining the normal redox potential of the body (Semprine et al., 2014). A decrease in the GSH/GSSG ratio is a potent indicator of oxidative stress as reported in a previous study (Shyam Verma and Srivastava, 2001). Chronic exposure of MWR significantly reduces the ratio of GSH/GSSG, which might be due to alteration in GSH cycle regulating enzymes (Sharma et al., 2020). The increased level of ROS is correlated with a decline in GPx activity, a crucial enzyme of the GSH cycle that plays an important role in the protection against hydrogen and lipid peroxides (Kivrak et al., 2017). MWR exposed animals showed a marked reduction in GPx activity (Sharma et al., 2021; 2020).

GR is a cytosolic hepatic enzyme involved in the replenishment of glutathione stores, it requires the presence of NADPH. Results showed a significant decline in GR activity that might be due to excessive utilization of its co-substrates such as NADPH to maintain the reduced form cellular GSH. These findings are also supported by various authors (Achudume et al., 2009; Kivrak et al., 2017).

The glutathione-S-transferase is a phase II enzyme that plays an important role to detoxify many DNA alkylating agents, carcinogens, and environmentally hazardous chemicals (Strange et al., 2000). In our experiments, lowering of neural GST activity was seen in MWR exposed animals, indicating the susceptibility of neurons to be attacked by a toxic electrophilic compound. The overproduction of free radicals might be associated with the depletion of GST activity (Ragy, 2015; Kesari et al., 2011).

Microglia are the brain's native immune cells, these are the phagocyte macrophages of the brain (Kofler and Wiley, 2011). MWR induced free radical may stimulate an immune response that initiates the activation of glial cells and the release of certain cytokines. In the present study, the inflammatory response was expressed by the uncontrolled release of pro and anti-inflammatory cytokines (Spooren et al., 2011). Overproduction of TNF-α, IL-6 and diminution of IL-10 has been associated with several clinical conditions directed to the neural damage. These results have been supported by Selmaoui and the group (Selmaoui et al., 2011). The release of inflammatory cytokines is also related to the genesis of brain white matter lesions (Yoon et al., 1997). As white matter refers to the areas of the central nervous system (CNS) that are mostly made up of myelinated axons, so directly or indirectly increase in the inflammatory cytokines may modulate the cell-to-cell communication in the brain, resulting in neurodegenerative diseases.

Previous studies also suggest that elevated inflammatory cytokines may cause significant damage to the brain (Ziebell and Morganti-kossmann, 2010; Merrill and Benveniste, 1996). The severity of MWR induced damage was confirmed by histopathological observations showing a significant decrease in the overall thickness of cerebellar cortex and molecular, granular layer of the hippocampus. Degenerated and pyknotic nuclei were also detected in the pyramidal and Purkinje cells of the brain. One of the previous studies also confirmed the pyknotic neuron cells in the brain of exposed mice with 1350, 1375 MHz frequency (Zymantiene et al., 2020). Radio waves increases the neurodegeneration, in the CA and DG regions through the excessive production of ROS, that finally leads to behavioral abnormalities in animals

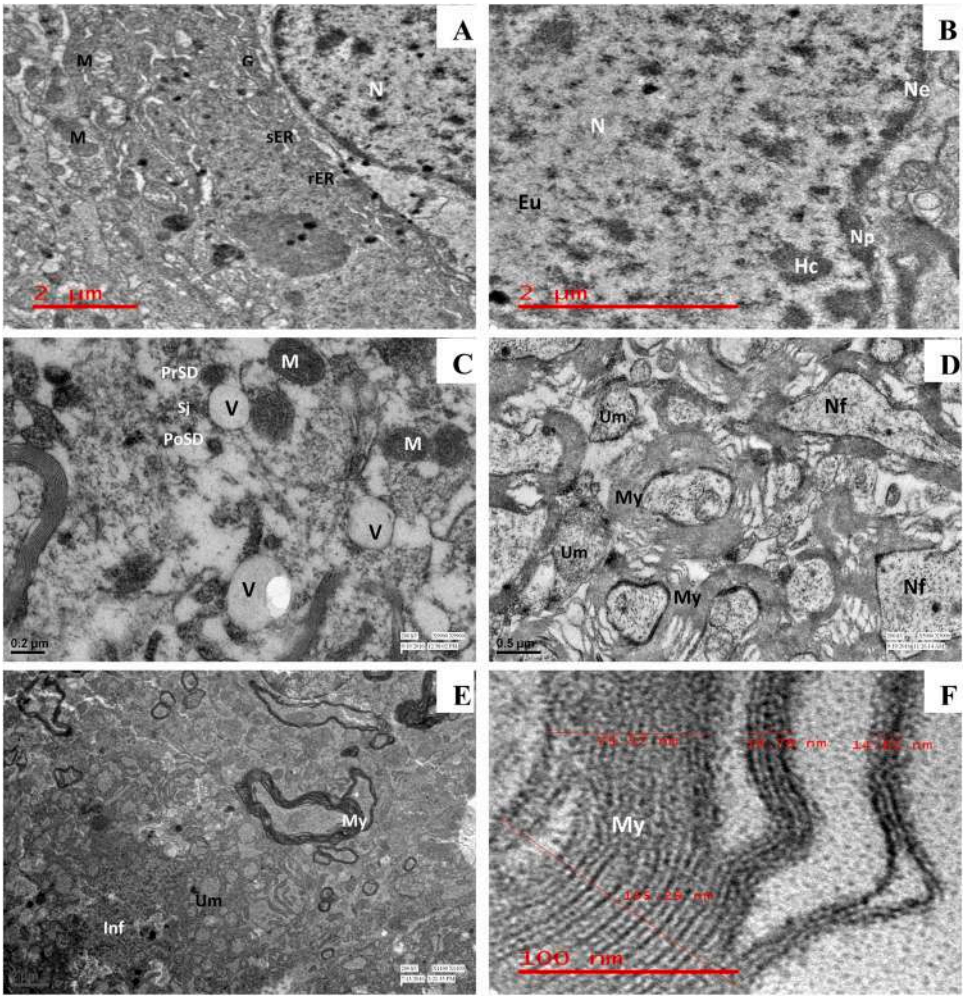


Fig. 9. Electron micrographs of MWR exposed animals. A–F: MWR exposed animals showed deformed nucleus (N) with an irregular arrangement of chromatin material, highly electron dense, unclear nuclear envelope (Ne), nuclear pore (Np) clumped channels of rough endoplasmic reticulum and Golgi bodies (G) and irregularly arranged condensed neurofilament (Nf). MWR exposure confirmed presence of heavy vacuolation (V) in neuron bodies, degenerated clumped mitochondria (M) along with unclear cristae (Cr), highly dense synaptic junctions (Sj), poor pre (Prsd) and post synaptic density (Posd). Demyelination in myelinated axons (My) with discontinued, wavy myelin sheath (My). Presence of autophagosomes (A) and appearance of inflammasome (Inf) was also confirmed.

that is reported in our previous study (Sharma et al., 2019). Our previous findings also confirmed that MWR exposure affected the muscular contraction that might be because of demyelination of CC region.

Corpus callosum (CC) plays an important role in the communication of both the hemispheres (Hinkley et al., 2016). There is a strong link between the integrity of corpus callosum white matter, the performance of neural conduction, and cognitive disability (Stricker et al., 2016; Patro et al., 2019). Thus, alteration in the CC-like demyelination reduced compaction or lesion directly correlated to neurological dysfunction (Amato et al., 2006). Chronically exposed animals showed demyelination in the corpus callosum followed by striatum, cauda putamen, and thalamus regions of the brain. It is already established that reduced compaction of corpus callosum interns the poor conduction and muscular contraction of MWR exposed animals (Sherafat et al., 2012; Granberg et al., 2014). The poor muscular contraction in case of MWR exposure was also observed in our previous study (Sharma et al., 2019).

Rapid nerve conduction is necessary for the sensory, motor, and cognitive functions of vertebrates. Axon myelination plays an important role in neuron cell conduction and signal processing contributing to proper brain functioning. The present study showed significant demyelination in the cortical neurons (Redmayne and Johansson, 2014; Kim et al., 2017). Our finding showed a deformed nucleus with the presence of degenerated mitochondria and presence of inflammasomes. The terminal synapses were loosely connected having a smaller number of synaptic vesicles. The findings substantiated previous research that claimed MWR caused cellular organelles to degrade by activating the autophagy pathway (Kim et al., 2017). Electron microscopic observations depict autophagosomes in the cerebral neurons followed by 90 days of microwave exposure. These results were verified by other groups showing the activation of the autophagy pathway in cortical neurons of the cerebral cortex (Kim et al., 2017). In a previous study, it has been also observed that 900 MHz frequency exposure to the brain up-regulates the apoptotic pathway (Köktürk et al., 2013). On the other hand, we have explored the myelin pattern of the axons and found that myelin sheaths were damaged, forming wavy and loose loops of myelin fibers. This was evident from other studies that established a connection between MWR induced myelin alteration as typical symptoms of demyelination-related Multiple Sclerosis and electro-hypersensitivity (Kim et al., 2017; Redmayne and Johansson, 2014).

5. Conclusion

In conclusion, our findings suggested that 2100 MHz frequency exposure (0.433, W/kg SAR) leads to an increase in free radicals due to compromised GSH homeostasis. It contributes to the poor defense capacity of the brain against reactive oxygen species that leads to a condition of oxidative stress. The oxidative stress modulates immune responses that further elicit neuronal cell death and demyelination. Thus, strengthening the statement that microwave radiation exposure is a "multi-hit" process of pathogenesis, including, oxidative stress, inflammatory activation, and demyelination contributed to the prevalence of neurodegenerative diseases.

6. Limitations and possible future developments

The present histopathological observations have some limitations which could be fulfilled in our future studies. In histopathological study we could have analyze synaptic junctions, it could have given more insight about the results. However, quantitative methods are still lacking for whole-brain analysis of pathological markers. The limitation of the myelin pathology is like SCoRe imaging could be used to quantify changes to compact myelin after exposure (Gonsalvez et al., 2019). In our future studies we would like to check whether chronic mobile phone exposure effects are reversible with above pathological analysis measures.

Ethics approval and consent to participate

No human subjects were used in the study. Experiments were conducted on laboratory animals (*Wistar* rats). Animals were maintained with the recommended ethical guidelines (1854/GO/Re/S/16/CPCSEA/IAEC/JU/24). The study was ethically approved by the Jiwaji University according to the Committee for the Purpose of Control and Supervision of Experiments on Animals (CPCSEA) guidelines.

Funding

This study was supported by the grant from University Grants Commission, India, meritorious fellowship (25-1/2014-15/(BSR)/7-97/2007/(BSR)-SSZ-1015/2015).

CRediT authorship contribution statement

Anjali Sharma: Writing – original draft, Writing – review & editing, Formal analysis, Investigation, Visualization, Conceptualization, Methodology, Funding acquisition. **Sangeeta Shukla:** Supervision. **Sadhana Shrivastava, Asha Singh, Shamli S. Gupte, Arti Rathore, Mohd Salim Reshi:** Data curation.

Code availability

Not applicable.

Author's Contribution

Sharma Anjali and Shukla Sangeeta designed the study. Sharma Anjali carried out the experimental, Writing – original draft, Writing – review & editing, Formal analysis, Investigation, Visualization, Conceptualization, Methodology, Funding acquisition. Shrivastava Sadhana, Singh Asha, Gupte Shamli S., Rathore Arti, and Reshi Mohd Salim helped in the Data curation. All authors read and approved the final manuscript.

Consent to participate

All authors meet the qualifications for authorship and had an opportunity to read and comment the manuscript.

Consent to publication

Not applicable.

Declaration of Competing Interest

The authors declare that they have no known competing financial interests or personal relationships that could have appeared to influence the work reported in this paper.

Availability of data and material

This manuscript has no associated data.

References

Achudume, A.C., Onibere, B., Aina, F., 2009. Bioeffects of electromagnetic base station on glutathione reductase, lipid peroxidation and total cholesterol in different tissues of Wistar rats. Biol. Med. 1, 33–38.

Adibhatla, R.M., J.F.H., 2007. Role of lipids in brain injury and diseases. ⟨https://doi.org/10.2217/17460875.2.4.403⟩.

Amato, M.P., Zipoli, V., Portaccio, E., 2006. Multiple sclerosis-related cognitive changes: a review of cross-sectional and longitudinal studies. J. Neurol. Sci. 245, 41–46. https://doi.org/10.1016/j.jns.2005.08.019.

Askar, M.A., Sumathy, K., Baquer, N.Z., 1996. Regulation and properties of purified glucose-6-phosphate dehydrogenase from rat brain. Indian J. Biochem. Biophys.

Bandara, P., Carpenter, D.O., 2020. Causes of cancer: perceptions vs. the scientific evidence. Eur. J. Cancer 124, 214–216. https://doi.org/10.1016/j.ejca.2019.08.036.

Banerjee, S., Singh, N.N., Sreedhar, G., Mukherjee, S., 2016. Analysis of the genotoxic effects of mobile phone radiation using buccal micronucleus assay: a comparative evaluation. J. Clin. Diagn. Res. 10, 82–85. https://doi.org/10.7860/JCDR/2016/17592.7505.

Berlin, A., Schaller, K.H., 1974. European standardized method for the determination of δ-aminolevulinic acid dehydratase activity in blood. Clin. Chem. Lab. Med. 12, 389–390. https://doi.org/10.1515/cclm.1974.12.8.389.

Bhatheja, K., Field, J., 2006. Schwann cells: origins and role in axonal maintenance and regeneration. Int J. Biochem. Cell Biol. 38, 1995–1999. https://doi.org/10.1016/j.biocel.2006.05.007.

Brown, H.D., Chattopadhyay, S.K., 1991. Ouabain inhibition of kidney ATPase is altered by 9.14 GHz radiation. Bioelectromagnetics 12, 137–143. https://doi.org/10.1002/bem.2250120302.

Chauhan, P., Verma, H.N., Sisodia, R., Kesari, K.K., 2017. Microwave radiation (2.45 GHz)-induced oxidative stress: whole-body exposure effect on histopathology of Wistar rats. Electromagn. Biol. Med. 36, 20–30. https://doi.org/10.3109/15368378.2016.1144063.

Clarke, P.G.H., 1984. Selective impregnation of developing neurons with the LOYEZ method and with two kinds of Luxol Fast Blue By. Acta Histochem. 74, 235–250. https://doi.org/10.1016/S0065-1281(84)80013-6.

D'Autréaux, B., Toledano, M.B., 2007. ROS as signalling molecules: mechanisms that generate specificity in ROS homeostasis. Nat. Rev. Mol. Cell Biol. 8, 813–824. https://doi.org/10.1038/nrm2256.

Deshmukh, P.S., Megha, K., Nasare, N., Banerjee, B.D., Ahmed, R.S., Abegaonkar, M.P., Tripathi, A.K., Mediratta, P.K., 2016. Effect of low level subchronic microwave radiation on rat brain. Biomed. Environ. Sci. 29, 858–867. https://doi.org/10.3967/bes2016.115.

Faridi, K., Khan, A.A., 2013. Effects of radiofrequency electromagnetic radiations (RF-EMR) on sector CA3 of hippocampus in albino rats–a light and electron-microscopic study. Curr. Neurobiol. 4, 13–18.

Fernandez-Fernandez, S., Bobo-Jimenez, V., Requejo-Aguilar, R., Gonzalez-Fernandez, S., Resch, M., Carabias-Carrasco, M., Ros, J., Almeida, A., Bolaños, J.P., 2018. Hippocampal neurons require a large pool of glutathione to sustain dendrite integrity and cognitive function. Redox Biol. 19, 52–61. https://doi.org/10.1016/j.redox.2018.08.003.

Freeman, L.C., Ting, J.P.Y., 2016. The pathogenic role of the inflammasome in neurodegenerative diseases. J. Neurochem. 136, 29–38. https://doi.org/10.1111/jnc.13217.

Gonsalvez, D.G., Yoo, S.W., Fletcher, J.L., Wood, R.J., Craig, G.A., Murray, S.S., Xiao, J., 2019. Imaging and quantification of myelin integrity after injury with spectral confocal reflectance microscopy. Front. Mol. Neurosci. 12, 1–13. https://doi.org/10.3389/fnmol.2019.00275.

Gorpinchenko, I., Nikitin, O., Banyra, O., Shulyak, A., 2014. The influence of direct mobile phone radiation on sperm quality. Cent. Eur. J. Urol. 67, 65–71. https://doi.org/10.5173/ceju.2014.01.art14.

Granberg, T., Martola, J., Bergendal, G., Shams, S., Damangir, S., Aspelin, P., Fredrikson, S., Kristoffersen-wiberg, M., 2014. Corpus callosum atrophy is strongly associated with cognitive impairment in multiple sclerosis: results of a 17-year longitudinal study. Mult. Scler. J. 21, 1–8. https://doi.org/10.1177/1352458514560928.

Griffiths, I., Klugmann, M., Anderson, T., Yool, D., Schwab, M.H., Schneider, A., Zimmermann, F., Mcculloch, M., Nadon, N., Nave, K., Griffiths, I., Klugmann, M., Anderson, T., Yool, D., Thomson, C., Schwab, M.H., Schneider, A., Zimmermann, F., Mcculloch, M., Nadon, N., Nave, K., 1998. Axonal Swellings and Degeneration in Mice Lacking the Major Proteolipid of Myelin Published by: American Association for the Advancement of Science Stable ⟨https://www.jstor.org/stable/2895967⟩ American Association for the Advancement of Science is c. Science (1979) 280, pp. 1610–3.

GSMA, 2020. GSMA. ⟨https://www.gsma.com⟩.

Gurer-orhan, H., Sabır, H.U., Özgüne, H., 2004. Correlation between clinical indicators of lead poisoning and oxidative stress parameters in controls and lead-exposed workers, vol. 195, pp. 147–54. ⟨https://doi.org/10.1016/j.tox.2003.09.009⟩.

Habig, W.H., Pabst, M.J., Jakoby, W.B., 1974. Glutathione S transferases. The first enzymatic step in mercapturic acid formation. J. Biol. Chem.

Haghani, M., Shabani, M., Moazzami, K., 2013. Maternal mobile phone exposure adversely affects the electrophysiological properties of Purkinje neurons in rat

offspring. Neuroscience 250, 588–598. https://doi.org/10.1016/j.neuroscience.2013.07.049.
Hayat, M.A., Giaquinta, R., 1970. Rapid fixation and embedding for electron microscopy. Tissue Cell 2, 191–195. https://doi.org/10.1016/S0040-8166(70)80015-5.
Hinkley, L.B.N., Marco, X.E.J., Brown, E.G., Bukshpun, P., Gold, J., Hill, S., Findlay, X.A. M., Jeremy, X.R.J., Wakahiro, M.L., Barkovich, X.A.J., Mukherjee, X.P., Sherr, X.E. H., Nagarajan, X.S.S., 2016. The contribution of the corpus callosum to language lateralization, vol. 36, pp. 4522–33. ⟨https://doi.org/10.1523/JNEUROSCI.3850-14.2016⟩.
Hissin, Hilf, 1976. A fluorometric method for determination of oxidized and reduced glutathione in tissues, vol. 226, pp. 214–26.
Ismaiil, L.A., Joumaa, W.H., Moustafa, M.E., 2019. Selenium decreases triglycerides and VLDL-c in diabetic rats exposed to electromagnetic radiation from mobile phone base stations. J. Taibah Univ. Sci. 13, 844–849. https://doi.org/10.1080/16583655.2019.1649881.
Israel, M., Vangelova, K., Ivanova, M., 2007. Cardiovascular risk under electromagnetic exposure in physiotherapy. Environmentalist 27, 539–543. https://doi.org/10.1007/s10669-007-9065-0.
Jangid, A.P., John, P.J., Yadav, D., Mishra, S., Sharma, P., 2012. Impact of chronic lead exposure on selected biological markers. Indian J. Clin. Biochem. 27, 83–89. https://doi.org/10.1007/s12291-011-0163-x.
Juutilainen, J., 2003. Developmental effects of extremely low frequency electric and magnetic fields. Radiat. Prot. Dosim. 106, 385–390. https://doi.org/10.1093/oxfordjournals.rpd.a006376.
Kesari, K.K., Kumar, S., Behari, J., 2011. 900-MHz microwave radiation promotes oxidation in rat brain. Electromagn. Biol. Med. 30, 219–234. https://doi.org/10.3109/15368378.2011.587930.
Kim, J.H., Yu, D.H., Huh, Y.H., Lee, E.H., Kim, H.G., Kim, H.R., 2017. Long-term exposure to 835 MHz RF-EMF induces hyperactivity, autophagy and demyelination in the cortical neurons of mice. Sci. Rep. 7. https://doi.org/10.1038/srep41129.
Kivrak, E., Yurt, K., Kaplan, A., Alkan, I., Altun, G., 2017. Effects of electromagnetic fields exposure on the antioxidant defense system. J. Microsc. Ultrastruct. 5, 167. https://doi.org/10.1016/j.jmau.2017.07.003.
Kofler, J., Wiley, C.A., 2011. Microglia: key innate immune cells of the brain. Toxicol. Pathol. 39, 103–114. https://doi.org/10.1177/0192623310387619.
Köktürk, S., Yardimoglu, M., Celikozlu, S.D., Dolanbay, E.G., Cimbiz, A., 2013. Effect of Lycopersicon esculentum extract on apoptosis in the rat cerebellum, following prenatal and postnatal exposure to an electromagnetic field. Exp. Ther. Med. 6, 52–56. https://doi.org/10.3892/etm.2013.1123.
Kumar, A., Tiwari, M., Ali, A., 2012. Evaluation of low blood lead levels and its association with oxidative stress in pregnant anemic women: a comparative prospective study. Indian J. Clin. Biochem. 27, 246–252. https://doi.org/10.1007/s12291-012-0202-2.
Lakroun, Z., Kebieche, M., Lahouel, A., 2015. Oxidative stress and brain mitochondria swelling induced by endosulfan and protective role of quercetin in rat. Environ. Sci. Pollut. Res. 22, 7776–7781. https://doi.org/10.1007/s11356-014-3885-5.
Li, Y., Shi, C., Lu, G., Xu, Q., Liu, S., 2012. Effects of electromagnetic radiation on spatial memory and synapses in rat hippocampal CA1. Neural Regen. Res. 7, 1248–1255. https://doi.org/10.3969/j.issn.1673-5374.2012.16.007.
Maines, M., 1980. Regional distribution of the enzymes of haem biosynthesis and the inhibition of 5-aminolevulinate synthase by manganese in the rat brain. Biochem. J. 190, 315–321.
Martínez-Sámano, J., Flores-Poblano, A., Verdugo-Díaz, L., Juárez-Oropeza, M.A., Torres-Durán, P.V., 2018. Extremely low frequency electromagnetic field exposure and restraint stress induce changes on the brain lipid profile of Wistar rats. BMC Neurosci. 19, 1–9. https://doi.org/10.1186/s12868-018-0432-1.
Merrill, J.E., Benveniste, E.N., 1996. Cytokines in inflammatory helpful and harmful, vol. 19, pp. 331–8.
Narayanan, S.N., Kumar, R.S., Potu, B.K., Nayak, S., Bhat, P.G., Mailankot, M., 2010. Effect of radio-frequency electromagnetic radiations (RF-EMR) on passive avoidance behaviour and hippocampal morphology in Wistar rats. Upsala J. Med. Sci. 115, 91–96. https://doi.org/10.3109/03009730903552661.
Narayanan, S.N., Mohapatra, N., John, P., Nalini, K., Kumar, R.S., Nayak, S.B., Bhat, P.G., 2018. Radiofrequency electromagnetic radiation exposure effects on amygdala morphology, place preference behavior and brain caspase-3 activity in rats. Environ. Toxicol. Pharm. 58, 220–229. https://doi.org/10.1016/j.etap.2018.01.009.
Oktem, F., Ozguner, F., Mollaoglu, H., Koyu, A., Uz, E., 2005. Oxidative damage in the kidney induced by 900-MHz-emitted mobile phone: Protection by melatonin. Arch. Med. Res. 36, 350–355. https://doi.org/10.1016/j.arcmed.2005.03.021.
Paglia, D.E., Valentine, W.N., 1967. Studies on the quantitative and qualitative characterization of erythrocyte glutathione peroxidase. J. Lab. Clin. Med. 70, 158–169. https://doi.org/10.5555/URI:PII:0022214367900765.
Panagopoulos, D.J., Johansson, O., Carlo, G.L., 2013. Evaluation of specific absorption rate as a dosimetric quantity for electromagnetic fields bioeffects. PLoS One 8, e62663. https://doi.org/10.1371/journal.pone.0062663.
Pareja-Peña, F., Burgos-Molina, A.M., Sendra-Portero, F., Ruiz-Gómez, M.J., 2020. Evidences of the (400 MHz to 3 GHz) radiofrequency electromagnetic field influence on brain tumor induction. Int. J. Environ. Health Res. 1–10. https://doi.org/10.1080/09603123.2020.1738352.
Pareja-Peña, F., Burgos-Molina, A.M., Sendra-Portero, F., Ruiz-Gómez, M.J., 2022. Evidences of the (400 MHz to 3 GHz) radiofrequency electromagnetic field influence on brain tumor induction. Int. J. Environ. Health Res. 32, 121–130. https://doi.org/10.1080/09603123.2020.1738352.
Patro, N., Naik, A.A., Patro, I.K., 2019. Developmental changes in oligodendrocyte genesis, myelination, and associated behavioral dysfunction in a rat model of intra-generational protein malnutrition, vol. 56, pp. 595–610.
Ragy, M.M., 2015. Effect of exposure and withdrawal of 900-MHz-electromagnetic waves on brain, kidney and liver oxidative stress and some biochemical parameters in male rats. Electromagn. Biol. Med. 34, 279–284. https://doi.org/10.3109/15368378.2014.906446.
Ravikumar Kurup, A., Parameswara Achutha, Kurup, 2012. Membrane sodium potassium atpase inhibition mediated Atp synthesis membrane sodium potassium ATPase inhibition mediated ATP synthesis induced by digoxin, photoinduction and electromagnetic fields. Adv. Nat. Sci. 5, 60–63. https://doi.org/10.3968/j.ans.1715787020120502.1458.
Redmayne, M., Johansson, O., 2014. Could myelin damage from radiofrequency electromagnetic field exposure help explain the functional impairment electrohypersensitivity? A review of the evidence. J. Toxicol. Environ. Health - Part B: Crit. Rev. 17, 247–258. https://doi.org/10.1080/10937404.2014.923356.
Salford, L.G., Brun, A.E., Eberhardt, J.L., Malmgren, L., Persson, B.R.R., 2003. Nerve cell damage in mammalian brain after exposure to microwaves from GSM mobile phones. Environ. Health Perspect. 111, 881–883. https://doi.org/10.1289/ehp.6039.
Selmaoui, B., Lambrozo, J., Sackett-Lundeen, L., Haus, E., Touitou, Y., 2011. Acute exposure to 50-Hz magnetic fields increases interleukin-6 in young healthy men. J. Clin. Immunol. 31, 1105–1111. https://doi.org/10.1007/s10875-011-9558-y.
Semprine, J., Ferrarotti, N., Musacco-Sebio, R., Saporito-Magriñá, C., Fuda, J., Torti, H., Castro-Parodi, M., Damiano, A., Boveris, A., Repetto, M.G., 2014. Brain antioxidant responses to acute iron and copper intoxications in rats. Metallomics 6, 2083–2089. https://doi.org/10.1039/c4mt00159a.
Seth, P.K., Tangri, K.K., 1966. Biochemical effects of some newer salicylic acid congeners. J. Pharm. Pharm. 18, 831–833. https://doi.org/10.1111/j.2042-7158.1966.tb07822.x.
Sharma, A., Sharma, S., Shrivastava, S., Singhal, P.K., Shukla, S., 2019. Mobile phone induced cognitive and neurochemical consequences. J. Chem. Neuroanat. 102, 101684 https://doi.org/10.1016/j.jchemneu.2019.101684.
Sharma, A., Shrivastava, S., Shukla, S., 2020. Exposure of radiofrequency electromagnetic radiation on biochemical and pathological alterations. Neurol. India 68, 1092–1100. https://doi.org/10.4103/0028-3886.294554.
Sharma, A., Shrivastava, S., Shukla, S., 2021. Oxidative damage in the liver and brain of the rats exposed to frequency-dependent radiofrequency electromagnetic exposure: biochemical and histopathological evidence. Free Radic. Res. 55, 535–546. https://doi.org/10.1080/10715762.2021.1966001.
Sherafat, M.A., Heibatollahi, M., Mongabadi, S., Moradi, F., Javan, M., Ahmadiani, A., 2012. Electromagnetic field stimulation potentiates endogenous myelin repair by recruiting subventricular neural stem cells in an experimental model of white matter demyelination. J. Mol. Neurosci. 48, 144–153. https://doi.org/10.1007/s12031-012-9791-8.
Shyam Verma, R., Srivastava, N., 2001. Chlorpyrifos induced alterations in levels of thiobarbituric acid reactive substances and glutathione in rat brain. Indian J. Exp. Biol. 39, 174–177.
Spooren, A., Kolmus, K., Laureys, G., Clinckers, R., De Keyser, J., Haegeman, G., Gerlo, S., 2011. Interleukin-6, a mental cytokine. Brain Res. Rev. 67, 157–183. https://doi.org/10.1016/j.brainresrev.2011.01.002.
Strange, R.C., Jones, P.W., Fryer, A.A., 2000. Glutathione S-transferase: genetics and role in toxicology. Toxicol. Lett. 112–113, 357–363. https://doi.org/10.1016/S0378-4274(99)00230-1.
Stricker, N.H., Salat, D.H., Kuhn, T.P., Foley, J.M., Price, J.S., Westlye, L.T., Esterman, M. S., Mcglinchey, R.E., Milberg, W.P., Leritz, E.C., 2016. Mild cognitive impairment is associated with white matter integrity changes in late-myelinating regions within the corpus callosum, 31, 68–75. https://doi.org/10.1177/1533317515578257.
Tayarani, I., Cloez, I., Clkment, M., Bourre, J., 1989. Antioxidant enzymes and related trace elements in aging brain capillaries and choroid plexus.
Volkow, N.D., Tomasi, D., Wang, G.J., Vaska, P., Fowler, J.S., Telang, F., Alexoff, D., Logan, J., Wong, C., 2011. Effects of cell phone radiofrequency signal exposure on brain glucose metabolism. JAMA – J. Am. Med. Assoc. 305, 808–813. https://doi.org/10.1001/jama.2011.186.
Wingerchuk, D.M., Lucchinetti, C.F., Noseworthy, J.H., 2001. Multiple sclerosis: current pathophysiological concepts. Lab. Investig. 81, 263–281.
Yoon, B.H., Jun, J.K., Romero, R., Park, H., Gomez, R., Choi, J., Kim, I., 1997. Amniotic fluid inflammatory cytokines (interleukin-6, interleukin-l [3, and tumor necrosis factor-s), neonatal brain white matter lesions, and cerebral palsy, vol. 177, pp. 19–26.
Yuan, X., Wang, Y., Li, L., Zhou, W., Tian, D., Lu, C., Yu, S., Zhao, J., Peng, S., 2016. PM2.5 induces embryonic growth retardation: potential involvement of ROS-MAPKs-apoptosis and G0/G1 arrest pathways. Environ. Toxicol. 31, 2028–2044. https://doi.org/10.1002/tox.22203.
Ziebell, J.M., Morganti-kossmann, M.C., 2010. Involvement of pro- and anti-inflammatory cytokines and chemokines in the pathophysiology of traumatic. Brain Inj. 7, 22–30.
Zymantiene, J., Juozaitiene, V., Zelvyte, R., Oberauskas, V., Spancerniene, U., Sederevicius, A., Aniuliene, A., 2020. Effect of electromagnetic field exposure on mouse brain morphological and histopathological profiling. J. Vet. Res. 64, 319–324. https://doi.org/10.2478/jvetres-2020-0030.